Available online at www.sciencedirect.com
ScienceDirect
Ceramics International 38S (2012) S467–S470
CERAMICS INTERNATIONAL
www.elsevier.com/locate/ceramint

Lithium ion migration pathways in $Li_{3x}La_{2/3-x}\square_{1/3-2x}TiO_3$

Dae-Hee Kim [a], Dae-Hyun Kim [a], Yong-Chan Jeong [a], Hwa-Il Seo [b], Yeong-Cheol Kim [a,*]

[a] Department of Materials Engineering, Korea University of Technology and Education, Cheonan 330-708, Republic of Korea
[b] School of Information Technology, Korea University of Technology and Education, Cheonan 330-708, Republic of Korea

Available online 14 May 2011

Abstract

We studied the Li^+ ion migration pathways in $Li_{3x}La_{2/3-x}\square_{1/3-2x}TiO_3$ at $x = 1/24$ using density functional theory. When four La atoms occupied the A-sites of the same layer (La-rich layer) and the remainder occupied the A-sites of another layer (La-poor layer), the structure was thermodynamically the most favorable. Because a Li^+ ion migrates through A-site vacancies, its migration in this structure occurs on the La-poor layer. There were two cavities through which the Li^+ ion could pass for long distance migration: between two La atoms (C_1) and within the center of the square that was formed by the four La atoms (C_2) in the La-poor layer. The Li^+ ion migrated around the A-site center from an off-centered favorable position to the symmetrical position at the C_1 site, and its energy barrier was 0.13 eV. Because the C_2 site was energetically unfavorable for the stay of the Li^+ ion, the Li^+ ion rotated at a right angle toward another C_1 site to avoid the C_2 site with the energy barrier of 0.24 eV. The results indicated that the Li^+ ion was conducted by the repetition of the transfer at the C_1 site and rotation near the C_2 site two-dimensionally on the La-poor layer, and the overall energy barrier for the lithium migration was 0.24 eV. We believe this value is reasonable, because the experimentally determined values in the range of 0.36–0.40 eV should consider migration through grain boundaries as well as through grains.

Keywords: C. Diffusion; D. Perovskites; E. Batteries; Density functional theory

1. Introduction

Solid state lithium ion batteries have been attracting lots of interest owing to their excellent properties of high power density and good safety. As a part of the battery, an inorganic solid state electrolyte becomes significant due to its exceptional capacity retention [1–3]. $Li_{3x}La_{2/3-x}\square_{1/3-2x}TiO_3$, which is one of perovskite oxides with an ABO_3 formula, has excellent electrical conductivity: $\sim 10^{-3}$ S/cm with $x = 0.1$ at room temperature [4–7]. It is known that the A-site vacancies of $Li_{3x}La_{2/3-x}\square_{1/3-2x}TiO_3$ provide the transport tunnels for Li^+ ion migration, and four neighboring TiO_6 octahedrons form the bottlenecks of these tunnels [8,9].

Studies of Li^+ ion migration in $Li_{3x}La_{2/3-x}\square_{1/3-2x}TiO_3$ using density functional theory (DFT) have been reported. Catti reported the Li^+ ion mobility pathways in $Li_{3x}La_{2/3-x}\square_{1/3-2x}TiO_3$ using CRYSTAL06 with B3LYP hybrid function [10]. They proposed two $Li_{3x}La_{2/3-x}\square_{1/3-2x}TiO_3$ models based on the segregation of the La vacancies; two La vacancies segregated in a layer (La-poor layer) were energetically more favorable than one La vacancy each distributed in two layers. However, when two La vacancies were positioned in the La-poor layer, the calculated energy barrier of 0.47 eV for the Li^+ ion was higher than the experimentally obtained ones, which were in the range of 0.36–0.40 eV [5,7,11–14]. They calculated the energy barrier by fixing the Li^+ ion and relaxing all the other atoms in the structure.

In the present paper, we studied the Li^+ ion migration pathways through the $Li_{3x}La_{2/3-x}\square_{1/3-2x}TiO_3$ superstructure at $x = 1/24$ using the climbing nudged elastic band (CNEB) tool that allowed all the atoms to be fully relaxed [15]. The calculated energy barriers were compared with the experimentally obtained ones.

2. Calculational

All calculations were performed using the Vienna *ab initio* simulation package (VASP) code with the projector augmented wave (PAW) potentials and generalized gradient approximation (GGA) [16–19]. The Li atom $2s^1$ state; La atom $5s^2$, $5p^6$, $5d^1$, and $6s^2$ states; Ti atom $3d^2$ and $4s^2$ states; and O atom $2s^2$ and

* Corresponding author. Tel.: +82 41 560 1326; fax: +82 41 560 1360.
E-mail address: yckim@kut.ac.kr (Y.-C. Kim).

0272-8842/$36.00 © 2011 Published by Elsevier Ltd and Techna Group S.r.l.
doi:10.1016/j.ceramint.2011.05.041

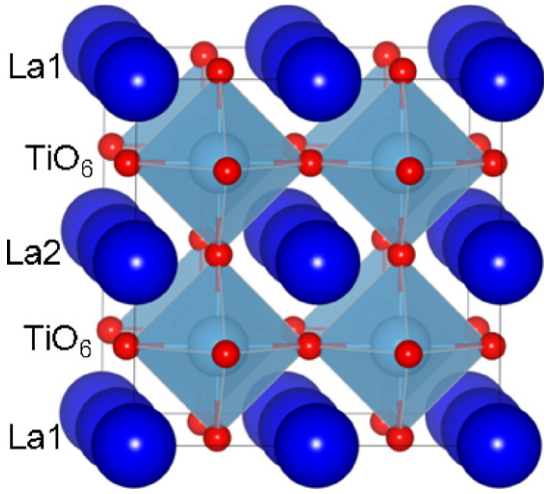

Fig. 1. Perspective view of the $Li_{3x}La_{2/3-x}\square_{1/3-2x}TiO_3$ structure along the [1 0 0] direction. La1 = La^{3+}, Li^+ or vacancy in the (0 0 0) plane and La2 = La^{3+}, Li^+ or vacancy in the (0 0 2) plane. Blue, light blue, and red spheres are the La, Ti, and O atoms, respectively. (For interpretation of the references to color in this figure legend, the reader is referred to the web version of the article.)

$2p^4$ states were treated as valence wave functions. The cutoff energy was 500 eV, and the *k*-points mesh was 4 × 4 × 4 using a Monkhorst–Pack grid method for bulk superstructures. The calculations were performed using the Gaussian method, non-spin polarized, and fully relaxed.

The unit cell of ABO_3 perovskite structure was expended to the 2 × 2 × 2 superstructure, as shown in Fig. 1. Four La and eight Ti atoms were positioned at the A- and B-sites, respectively. Three La atoms were removed, and then a Li^+ ion was added to the superstructure. Therefore, the structure consisted of five La atoms, two A-site vacancies, one Li^+ ion, and eight TiO_6 octahedrons per orthorhombic $a(\sim 2a_p) \times b(\sim 2a_p) \times c(\sim 2a_p)$ unit cell. After the optimization of the structure, we calculated the energy barriers for the Li^+ ion migration using the CNEB tool implemented in the VASP code [15]. All transition states in the Li^+ ion migration were relaxed for the energy barrier calculations.

3. Results and discussion

We considered the arrangements of the La atoms and Li^+ ion at A-sites of the $Li_{3x}La_{2/3-x}\square_{1/3-2x}TiO_3$ unit cell at $x = 1/24$. Fig. 2(a) and (b) shows that one and four La atoms are located in the La1- and La2-layers, respectively, and Fig. 2(c)–(f) shows that two and three La atoms are located in the La1- and La2-layers, respectively. When four La atoms occupied the A-sites of the La1-layer (La-rich) and the remainder occupied the A-sites of the La2-layer (La-poor), as shown in Fig. 2(a), two A-site vacancies were positioned near the Li^+ ion in the La-poor layer. Its relative energy was set to 0.00 eV as a reference. The relative energy was increased to 0.46 eV when the Li^+ ion was located near the La atoms diagonally, as shown in Fig. 2(b). When the Li^+ ion was located at different sites in the structure, as shown in Fig. 2(c)–(f), the energies were 0.98, 0.51, 1.47, and 0.65 eV, respectively. Therefore, the structure of the Li^+ ion located between the two La atoms on the La-poor layer (Fig. 2(a)) was chosen for the energy barrier calculations of the Li^+ ion, because the structure was energetically the most favorable. The Li^+ ion was further moved near an O atom and above or below the La-poor layer. In this case, the relative energy was decreased to −0.76 eV due to the interaction between the O atom and the Li^+ ion located at the A-site vacancy. This result is well matched to the literature [20].

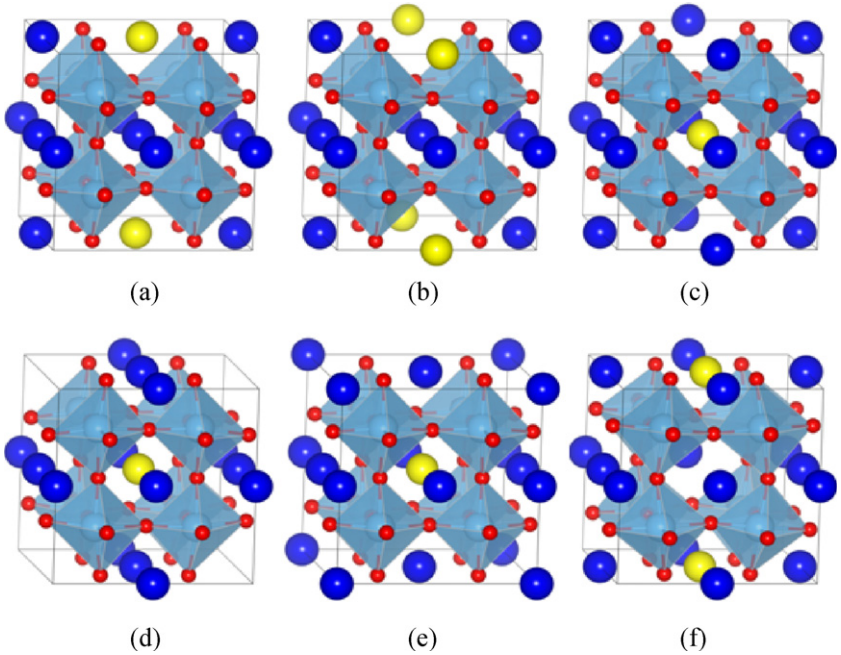

Fig. 2. Perspective views of possible atom arrangements of the A-site in $Li_{3x}La_{2/3-x}\square_{1/3-2x}TiO_3$ along the [1 0 0] direction. The energy was set to 0 eV as a reference when four La atoms were located in a layer and one Li^+ ion was located between two La atoms in the La-poor layer.

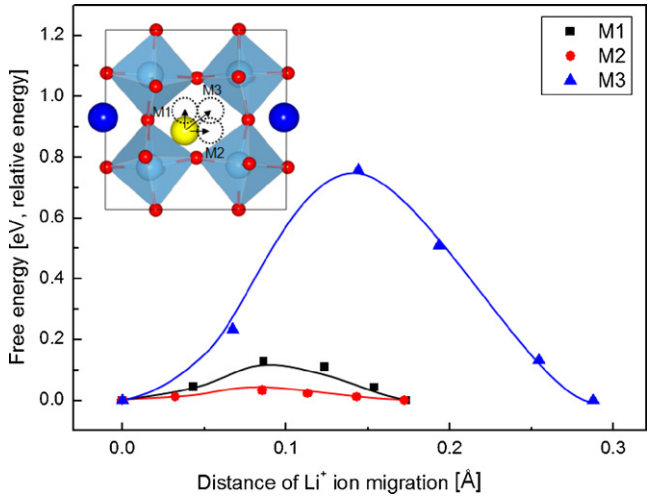

Fig. 3. The energy variation as a function of the Li^+ ion migration distance. Small inset shows that planar view of the Li^+ ion migration on the La-poor layer along [0 0 1] direction. M1, M2, and M3 indicate the $L1^+$ ion migration to the neighboring same sites along the [1 0 0], [0 1 0], and [1 1 0] directions, respectively.

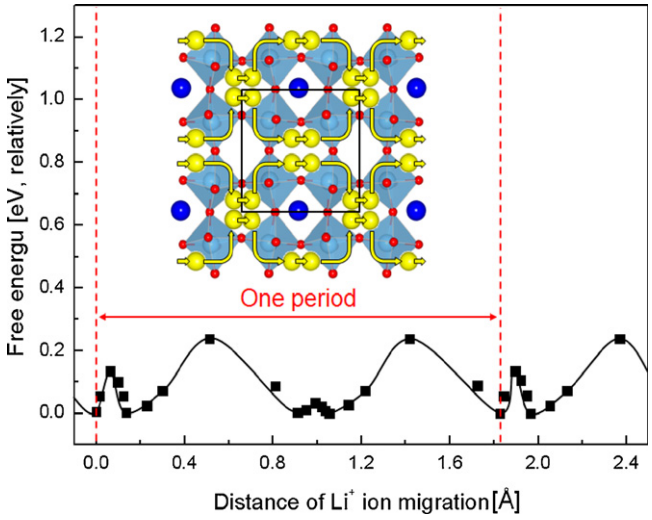

Fig. 5. The energy barrier for Li^+ ion migration through the $Li_{3x}La_{2/3-x}\square_{1/3-2x}TiO_3$ along the [1 0 0] direction. Planar view is shown along the [0 0 1] direction in small inset.

Since two A-site vacancies were positioned near the Li^+ ion, the Li^+ ion could migrate through the vacancies on the La-poor layer. The La-poor layer has four equivalent sites for the Li^+ ion in the $Li_{3x}La_{2/3-x}\square_{1/3-2x}TiO_3$ unit cell at $x = 1/24$, as shown in small inset in Fig. 3. M1, M2, and M3 indicate the Li^+ ion's migration to the neighboring equivalent sites along the [1 0 0], [0 1 0], and [1 1 0] directions, respectively. Fig. 3 shows the relative energy variation as a function of the Li^+ ion migration distance along the three directions. In the cases of M1 and M2, energy barriers for the Li^+ ion migration were 0.13 and 0.03 eV, respectively. However, a high energy barrier of 0.76 eV was needed for Li^+ ion migration along the [1 1 0] direction. Namely, the Li^+ ion located at the A-site vacancy could migrate easily in a straight line with the low energy barriers between the two La atoms on the La-poor layer.

We considered the Li^+ ion migration through the A-site vacancies on the La-poor layer in $Li_{3x}La_{2/3-x}\square_{1/3-2x}TiO_3$ at $x = 1/24$. There are two cavities on the La-poor layer. C_1 and C_2 indicate the cavities between two La atoms and among four La atoms, respectively. We calculated the energy barriers for the Li^+ ion migration from one C_1 site to another C_1 site with (red dotted line) and without (red solid line) passing through a C_2 site. A high energy barrier of 1.19 eV was needed for the Li^+ ion transfer from a C_1 site to another C_1 site passing through a C_2 site directly, because the relative energy was increased at the C_2 site, as shown in small inset in Fig. 4. However, a relatively low energy barrier of 0.24 eV was needed for the Li^+ ion rotation by 90° from a C_1 site to another C_1 site without passing through a C_2 site, as shown in Fig. 4. Therefore, the Li^+ ion can migrate via the rotation in the La-poor layer of $Li_{3x}La_{2/3-x}\square_{1/3-2x}TiO_3$ at $x = 1/24$.

Small inset in Fig. 5 shows the pathways for the Li^+ ion migration along the [1 0 0] direction in the $2 \times 2 \times 2$ $Li_{3x}La_{2/3-x}\square_{1/3-2x}TiO_3$ superstructure at $x = 1/24$. The Li^+ ion easily transferred in the C_1 site in a straight line with the low energy barrier of 0.03 eV, as shown in Fig. 5. In addition, it rotated by 90° between the two C_1 sites with a low energy barrier of 0.24 eV, while the Li^+ ion could not migrate through the C_2 site because the high energy barrier of 1.19 eV was needed on the La-poor layer. Therefore, since the Li^+ ion migration is composed of the combination of transfer and rotation, the energy barrier of 0.24 eV was chosen for long distance Li^+ ion migration. This value is lower than that of experimentally obtained values in the range of 0.36–0.40 eV, because grain boundaries typically observed in experimental samples can impede Li^+ ion further [21–23]. Therefore, we believe the energy barrier of 0.24 eV is reasonable for Li^+ ion migration through grains.

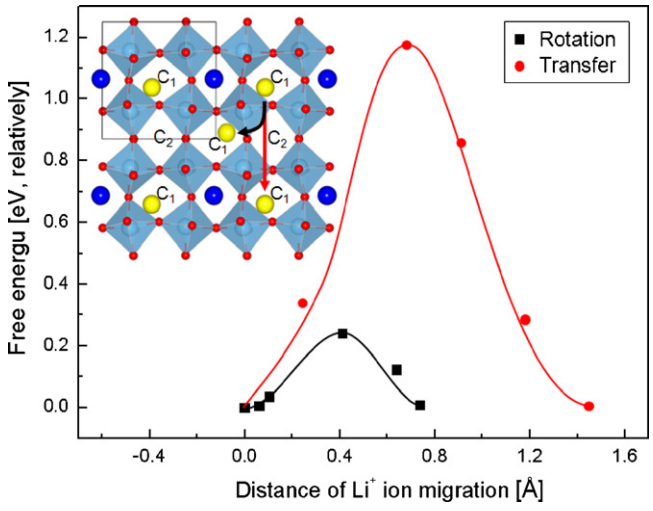

Fig. 4. The energy variation as a function of the Li^+ ion migration distance. Planar view of the Li^+ ion rotation (black line) and transfer (red line) in $Li_{3x}La_{2/3-x}\square_{1/3-2x}TiO_3$ is shown along the [0 0 1] direction in small inset. (For interpretation of the references to color in this figure legend, the reader is referred to the web version of the article.)

4. Conclusions

We calculated the energy barriers for Li^+ ion migration in a $Li_{3x}La_{2/3-x}\square_{1/3-2x}TiO_3$ unit cell at $x = 1/24$ using density functional theory. The four La atoms positioned on the La-rich layer and two A-site vacancies and the one Li^+ ion positioned on the La-poor layer were energetically the most favorable. The Li^+ ion easily migrated in the cavity located between the two La atoms with low energy barriers in the range of 0.03–0.13 eV on the La-poor layer. However, a high energy barrier of 1.19 eV was needed for Li^+ ion migration through the cavity located in the center of the four La atoms on the La-poor layer. The Li^+ ion rotated by 90° with a low energy barrier of 0.24 eV to migrate from a cavity between two La atoms to another equivalent cavity without passing through a cavity located in the center of the four La atoms. We believe that our calculated value of 0.24 eV is reasonable because the experimental values should consider migration through grain boundaries as well as through grains.

Acknowledgement

This work was supported by Korea University of Technology and Education Research Grant 2010.

References

[1] P. Knauth, H.L. Tuller, Solid-state ionics: roots, status, and future prospects, J. Am. Ceram. Soc. 85 (2002) 1654–1680.

[2] T. Takeuchi, K. Ado, Y. Saito, M. Tabuchi, H. Kageyama, O. Nakamura, Effect of tetragonal content of $BaTiO_3$ particles on the ionics conductivity enhancement in a $Na_4Zr_2Si_3O_{12}/BaTiO_2$ composite electrolyte, Solid State Ionics 89 (1996) 345–349.

[3] H. Aono, E. Sugimoto, Y. Sadaoka, N. Imanaka, G. Adachi, Electrical property and sinterability of $LiTi_2(PO_4)_3$ mixed with lithium salt (Li_3PO_4 or Li_3BO_3), Solid State Ionics 47 (1991) 257–264.

[4] A.G. Belous, G.N. Novitskaya, S.V. Polyanetskaya, Y.I. Gornikov, Investigation of complex oxides of the composition $La_{2/3-x}Li_{3x}TiO_3$, Neorgan. Mater. 23 (1987) 470–472.

[5] Y. Inaguma, C. Liquan, M. Itoh, T. Nakamura, T. Uchida, H. Ikuta, M. Wakihara, High ionic conductivity in lithium lanthanum titanate, Solid State Commun. 86 (1993) 689–693.

[6] H. Kawai, J. Kuwano, Lithium ion conductivity of A-site deficient perovskite solid solution $La_{0.67-x}Li_{3x}TiO_3$, J. Electrochem. Soc. 141 (1994) L78–L79.

[7] Y. Inagumi, L. Chen, M. Itoh, T. Nakamura, Candidate compounds with perovskite structure for high lithium ionic conductivity, Solid State Ionics 70 (1994) 196–202.

[8] O. Bohnke, J. Emery, A. Veron, J.L. Fourquet, J.Y. Buzare, P. Florian, D. Massiot, A distribution of activation energies for the local and long-range ionic motion is consistent with the disordered structure of the perovskite $Li_{3x}La_{2/3-x}TiO_3$, Solid State Ionics 109 (1998) 25–34.

[9] M. Nakayama, H. Ikuta, Y. Uchimoto, M. Wakihara, Ionic conduction of lithium in B-site substituted perovskite compounds, $(Li_{0.1}La_{0.3})_yM_xNb_{1-x}O_3$ (M = Zr, Ti, Ta), J. Mater. Chem. 12 (2002) 1500–1504.

[10] M. Catti, Ion mobility pathways of the Li^+ conductor $Li_{0.125}La_{0.625}TiO_3$ by ab initio simulations, J. Phys. Chem. C 112 (2008) 11068–11074.

[11] G.Y. Adachi, N. Imanaka, H. Aono, Fast Li⊕ conducting ceramic electrolytes, Adv. Mater. 8 (1996) 127–135.

[12] S. Stramare, V. Thangadurai, W. Weppner, Lithium lanthanum titanates: a review, Chem. Mater. 15 (2003) 3974–3990.

[13] J.A. Alonso, J. Sanz, J. Santamaria, C. Leon, A. Varez, M.T. Fernandez-Diaz, On the location of Li^+ cations in the fast Li-cation conductor $La_{0.5}Li_{0.5}TiO_3$ perovskite, Angew. Chem. Int. Ed. 39 (2000) 619–621.

[14] J. Emery, J.Y. Buzare, O. Bohnke, J.L. Fourquet, Lithium-7 NMR and ionic conductivity studies of lanthanum lithium titanate electrolytes, Solid State Ionics 99 (1997) 41–51.

[15] D. Sheppard, R. Terrell, G. Henkelman, Optimization methods for finding minimum energy paths, J. Chem. Phys. 128 (2008) 134106–134115.

[16] G. Kresse, J. Furthüller, Efficiency of ab-initio total energy calculations for metals and semiconductors using a plane-wave basis set, Comput. Mater. Sci. 6 (1996) 15–50.

[17] G. Kresse, J. Furthüller, Efficient iterative schemes for *ab initio* total-energy calculations using a plane-wave basis set, Phys. Rev. B 54 (1996) 11169–11186.

[18] G. Kresse, D. Joubert, From ultrasoft pseudopotentials to the projector augmented-wave method, Phys. Rev. B 59 (1999) 1758–1775.

[19] D. Vanderbilt, Soft self-consistent pseudopotentials in a generalized eigenvalue formalism, Phys. Rev. B 41 (1990) 7892–7895.

[20] Y. Inaguma, Y. Matsui, J. Yu, Y.-J. Shan, T. Nakamura, M. Itoh, Effect of substitution and pressure on lithium ion conductivity in perovskites $Ln_{1/2}Li_{1/2}TiO_3$ (Ln = La, Pr, Nd, and Sm), J. Phys. Chem. Solids 58 (1997) 843–852.

[21] O. Bohnke, The fast lithium-ion conducting oxides $Li_{3x}La_{2/3-x}TiO_3$ from fundamentals to applications, Solid State Ionics 179 (2008) 9–15.

[22] A. Morata-Orrantia, S. García-Martín, M.Á. Alario-Franco, New $La_{2/3-x}Sr_xLi_xTiO_3$ solid solution: structures, microstructures, and Li^+ conductovoty, Chem. Mater. 15 (2003) 363–367.

[23] S. García-Martín, M.Á. Alario-Franco, H. Ehrenberg, J. Rodríguez-Carvajal, U. Amador, Crystal structure and microstructure of some $La_{2/3-x}Li_{3x}TiO_3$ oxides: an example of the cpmplementary use of electron diffraction and microscopy and synchrotron X-ray diffraction to study complex materials, J. Am. Chem. Soc. 126 (2004) 3587–3596.